

Cite this: *Chem. Sci.*, 2024, 15, 5319

All publication charges for this article have been paid for by the Royal Society of Chemistry

# Combining total synthesis and genetic engineering to probe dihydropyran formation in ambruticin biosynthesis†

James I. Bowen,<sup>‡a</sup> Xiaotong Zhong,<sup>‡b</sup> Kaining Gao,<sup>‡bc</sup> Benjamin Reed,<sup>a</sup> Matthew P. Crump,<sup>‡a</sup> Luoyi Wang<sup>‡\*b</sup> and Christine L. Willis<sup>‡\*a</sup>

The ambruticins are a family of potent antifungal polyketide derived natural products isolated from the myxobacterium *Sorangium cellulosum*. Their unusual structures include a trisubstituted cyclopropyl group and two oxygen heterocycles, a tetrahydropyran (THP) and dihydropyran (DHP). Herein we report a flexible modular approach for the total synthesis of ambruticins which is used to prepare ambruticins F and S as well as in the first total synthesis of 20,21-dihydroambruticin F. The flexible strategy unites 3 fragments via Julia–Kocienski olefinations and provides important standards for investigation of dihydropyran formation in ambruticin biosynthesis. Cultures of wild-type *S. cellulosum* So ce10 produce mainly ambruticin S and the VS series of metabolites. An efficient electroporation method enabled gene knockout experiments which revealed that the  $\Delta ambP$ -S mutant of *S. cellulosum* accumulated the bisTHP polyketide 20,21-dihydroambruticin F. In contrast, the  $\Delta ambN$ -S mutant gave ambruticin F with the 20,21-alkene as the major metabolite confirming that AmbP and AmbO (a Rieske enzyme and flavin-dependent monooxygenase respectively) are implicated in 20,21-alkene formation. The results of feeding studies to a *Sorangium* strain containing only *ambP* and *ambO* are in accord with formation of the 20,21-alkene occurring prior to generation of the C3 to C7 dihydroxylated tetrahydropyran in ambruticin biosynthesis.

Received 30th January 2024  
Accepted 27th February 2024

DOI: 10.1039/d4sc00720d

rsc.li/chemical-science

## Introduction

The ambruticins (*e.g.* ambruticins F and S) are a family of polyketide derived natural products, isolated from the myxobacterium *Sorangium (Polyangium) cellulosum* (Scheme 1).<sup>1,2</sup> They exhibit potent antifungal activity against a range of fungal pathogens including *Coccidioides immitis* and *Blastomyces dermatitidis*.<sup>3,4</sup> Their antimycotic activity originates from interaction with the high-osmolarity glycerol (HOG) protein kinase signalling pathway.<sup>5</sup> Importantly, no toxicity was observed in mice dosed with ambruticin S.<sup>6</sup> Antifungal resistance is an area of growing concern which poses a severe threat to public health and food security.<sup>7–10</sup> Global warming has exacerbated this by fuelling the worldwide spread of fungi.<sup>11,12</sup> Research into lead compounds such as the ambruticins has been stimulated by the

urgent need to develop antimycotics with novel modes of action to address antifungal resistance.<sup>13</sup>

The ambruticins share several key structural features including a tetrahydropyran (THP) and dihydropyran (DHP) with a hydrocarbon linker incorporating an unusual trisubstituted cyclopropyl ring and 4 olefinic bonds. The structures of the major metabolites from *S. cellulosum* differ at C-5 and include an alcohol (ambruticin S) or amines such as ambruticins VS-5 and VS-4 (Scheme 1A). Ambruticin F (2), the C-5 epimer of ambruticin S (4), has been isolated as a minor metabolite, however, spectral data were not recorded.<sup>14</sup> Total syntheses of just two members of this family of natural products, ambruticin S and ambruticin J, have been described.<sup>15–21</sup>

In 2006, Reeves reported analysis of the ambruticin biosynthetic gene cluster (BGC) and proposed several unusual features of the modular biosynthetic pathway based on the results from isotopic labelling studies alongside gene knockout experiments.<sup>22</sup> In the tailoring phase of the polyketide pathway, the THP ring is proposed to be formed by the AmbJ catalysed 6,7-epoxidation of ambruticin J (1), followed by selective intramolecular attack on the oxirane ring to afford ambruticin F (2) (Scheme 1A).<sup>22,24</sup> AmbQ and AmbN are implicated in oxidation of 2 to 5-ketoambruticin (3), and subsequent reduction to ambruticin S (4). In a parallel pathway reductive amination of ketone 3 (by AmbR) was proposed to give ambruticin VS-5 (5),

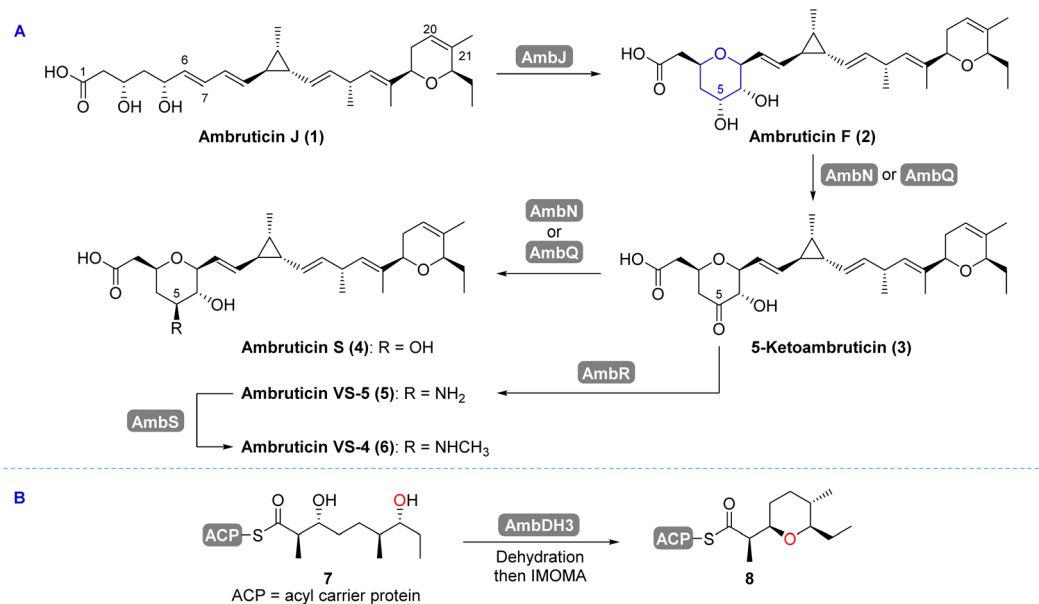
<sup>a</sup>School of Chemistry, University of Bristol, Bristol, BS8 1TS, UK. E-mail: chris.Willis@bristol.ac.uk

<sup>b</sup>Institute of Microbiology, Chinese Academy of Sciences, No. 1 Beichen West Road, Chaoyang District, Beijing 100101, China. E-mail: wangluoyi@im.ac.cn

<sup>c</sup>School of Life Sciences, Yunnan University, Kunming 650500, China

† Electronic supplementary information (ESI) available: Gene knockout procedures, synthetic procedures and NMR spectra. See DOI: <https://doi.org/10.1039/d4sc00720d>

‡ These authors contributed equally



**Scheme 1** (A) Proposed late stage transformations in ambruticin biosynthesis.<sup>22</sup> (B) Dehydration and intramolecular oxa-Michael addition (IMOMA) generates an intermediate in the biosynthesis of the DHP.<sup>22,23</sup>

which undergoes *N*-methylation (by AmbS) to deliver ambruticin VS-4 (6).

The biosynthetic origin of the DHP ring of the ambruticins is unusual. Hahn and co-workers revealed that the oxygen heterocycle is initially formed from linear polyketide 7 by AmbDH3 catalysed dehydration and subsequent intramolecular oxa-Michael addition (IMOMA) giving THP 8 (Scheme 1B).<sup>23</sup> AmbDH3 has broad substrate specificity as demonstrated in its use in the chemoenzymatic synthesis of the diarylheptanoid centrolbine.<sup>25</sup> The results of gene knockout experiments led Reeves to propose that dehydrogenation of the THP to a DHP occurs later in the biosynthetic pathway, catalysed by the Rieske oxygenase AmbP and the NAD(P)/FAD-dependent oxidoreductase AmbO.<sup>22</sup> LC-MS analysis of culture extracts of mutants of *S. cellulorum* where *ambP* or *ambO* were disrupted indicated that a series of 20,21-dihydroambruticins was produced at similar relative levels to each of the corresponding ambruticins (with the 20,21-alkene) found in the wild-type strain.<sup>22</sup> Hence selective desaturation may occur at various points in the biosynthetic pathway. However, no NMR spectral data for the bisTHP products were reported. Herein we describe the total syntheses of both 20,21-dihydroambruticin F (9) and ambruticin F (2) alongside the results of gene knockout experiments, giving the first definitive experimental evidence for desaturation catalysed by AmbP and AmbO in ambruticin biosynthesis.

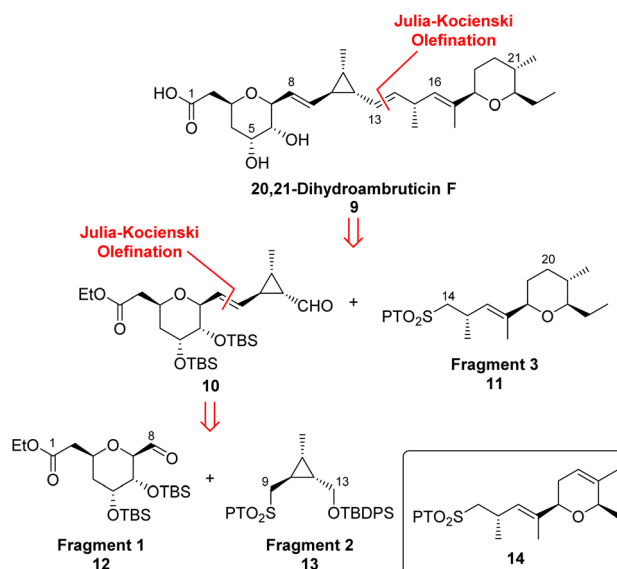
## Results and discussion

### Total syntheses of 20,21-dihydroambruticin F, ambruticin F and ambruticin S

As 20,21-dihydroambruticin F (9) is novel and no literature NMR data are available for ambruticin F (2), we required authentic samples of both to confirm the structures of accumulated

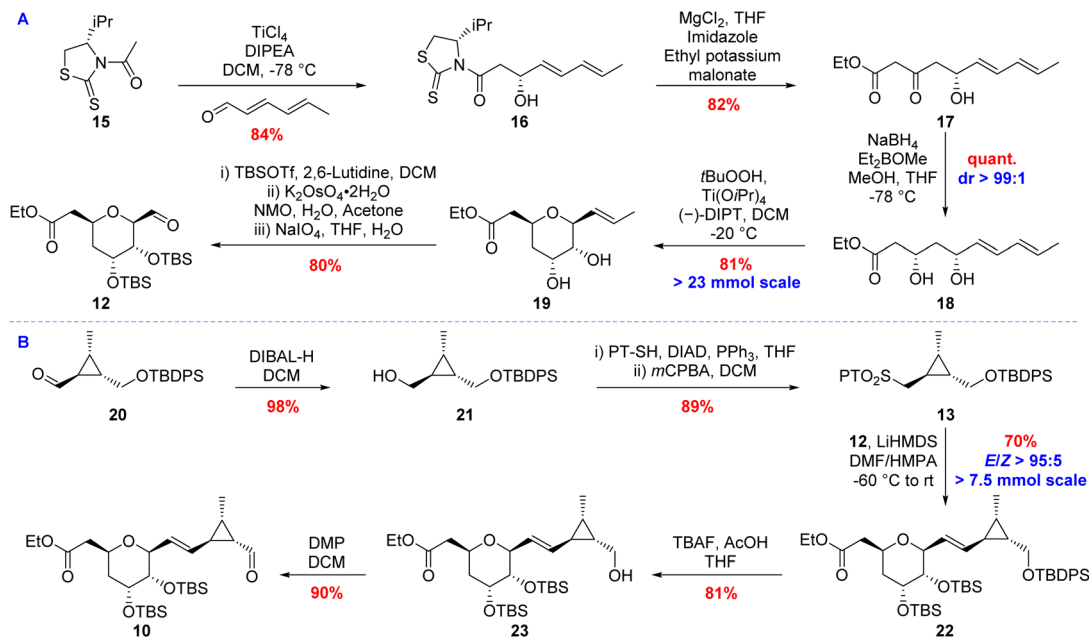
products in our proposed gene knockout experiments.<sup>14</sup> First the total synthesis of 20,21-dihydroambruticin F was investigated based on a flexible modular approach whereby three fragments 11, 12 and 13 were to be united by two Julia-Kocienski olefinations (Scheme 2).<sup>26</sup> This synthetic strategy would then be readily adapted for the synthesis of ambruticin F by using the DHP containing sulfone 14 rather than the saturated oxygen heterocycle 11 as a coupling partner.

The C1–C8 fragment (12) was prepared *via* a bioinspired epoxidation–cyclisation cascade based on the proposed selective THP formation in the AmbJ catalysed conversion of ambruticin J to ambruticin F (Scheme 1A).<sup>20</sup> Asymmetric aldol condensation



**Scheme 2** Retrosynthetic analysis of 20,21-dihydroambruticin F (9).





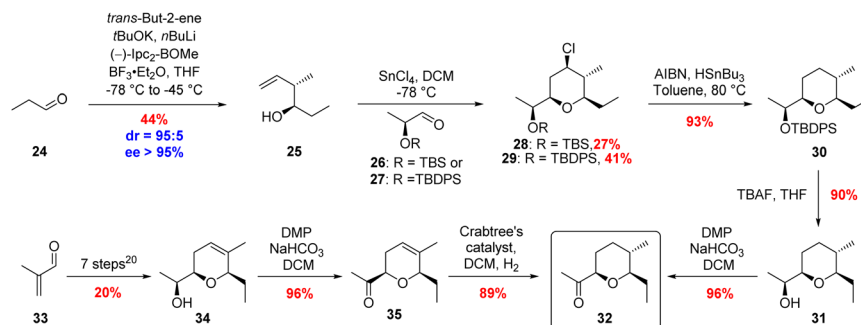
Scheme 3 (A) Synthesis of aldehyde 12. (B) Synthesis of aldehyde 10.

between *E,E*-hexadienal and acetylthiazolidinethione **15**, followed by a decarboxylative Claisen condensation gave  $\beta$ -hydroxy ketone **17** (Scheme 3A).<sup>27</sup> Stereoselective Narasaka–Prasad reduction of **17** yielded *syn*-diol **18** in 69% yield over the three steps. The *syn*-diol relationship was confirmed by Rychnovsky analysis of the corresponding acetone (see ESI†).<sup>28–30</sup> Conversion of 3,5-dihydroxy ester **18** to THP **19** was achieved *via* Sharpless asymmetric epoxidation, with the intermediate epoxide undergoing selective spontaneous cyclisation, providing THP **19** in 81% yield.<sup>24,31</sup> These reactions could be readily conducted on >23 mmol scale. Protection of the *syn*-diol as silyl ethers followed by oxidative cleavage of the alkene afforded the desired aldehyde fragment **12** in 45% yield over 6 steps from **15**.

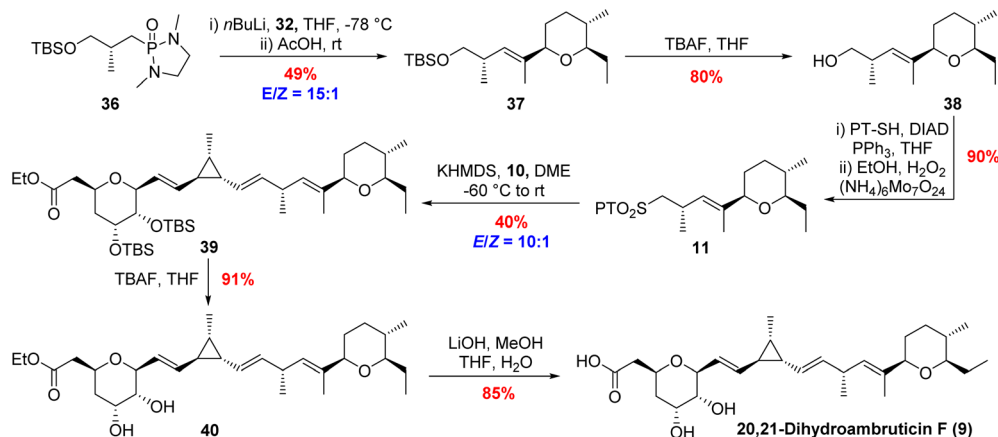
For the C9–C13 fragment (**13**), reduction of the known aldehyde **20** (ref. 20) with DIBAL-H followed by a Mitsunobu reaction and oxidation with *m*CPBA provided the phenyl tetra-sulfone **13** (Scheme 3B).<sup>17</sup> Oxidation of the intermediate sulfide was also achieved using molybdate and H<sub>2</sub>O<sub>2</sub> in ethanol giving similar yields of sulfone **13**, but the reaction proved less

amenable to scale up.<sup>32</sup> Julia–Kocienski reaction of aldehyde **12** with sulfone **13** afforded the desired *E*-olefin **22** in 70% yield. LiHMDS in a mixture of DMF and HMPA was required to achieve the required *trans*-selectivity in the reaction, which was conducted successfully on >7.5 mmol scale.<sup>17</sup> Selective deprotection of the primary alcohol with TBAF and acetic acid in THF followed by oxidation with Dess–Martin periodinane (DMP) furnished aldehyde **10** in 73% yield over the two steps.<sup>33</sup>

The final building block required for the total synthesis of 20,21-dihydroambruticin **F** (**9**) was tetrahydropyran **11**. Prins cyclisations have been widely used in natural product synthesis and we investigated the use of a SnCl<sub>4</sub> mediated Prins cyclisation for the stereoselective construction of the THP ring.<sup>34,35</sup> Reaction of homoallylic alcohol **25** with 2-*tert*-butyldimethylsilyloxypropanal **26**, gave THP **28** with all four substituents in the required equatorial position but in a disappointing 27% yield due to *in situ* deprotection of the silyl ether (Scheme 4). Using the more robust TBDPS protecting group gave **29** in 41% yield. Radical dechlorination of **29** followed by deprotection of the



Scheme 4 Two approaches to the synthesis of ketone 32.



Scheme 5 Synthesis of sulfone **11** and completing the total synthesis of 20,21-dihydroambruticin F (**9**).

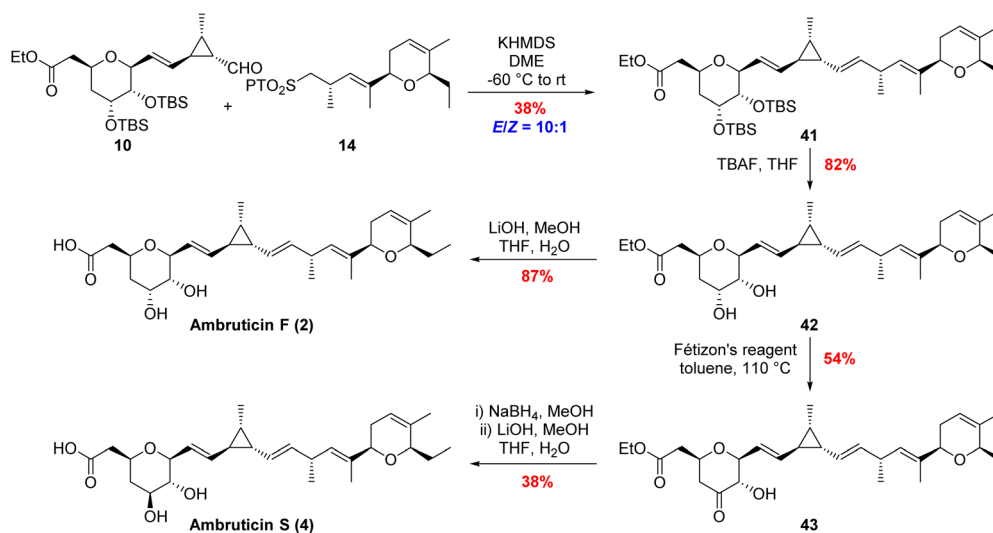
silyl ether and subsequent oxidation of the resultant alcohol gave ketone **32** in 80% yield over the 3 steps from **29**.<sup>35</sup>

An alternative approach to ketone **32** began with the known DHP **34** prepared in 7 steps and 20% overall yield from **33**.<sup>20,36</sup> Following oxidation of **34**, hydrogenation of **35** with Crabtree's catalyst afforded the desired THP fragment **32** in 89% yield as a single diastereomer (Scheme 4).<sup>37</sup> The observed selectivity was rationalised by hydrogenation being directed to the top face of the alkene by the ketone.

Ketone **32** was coupled with known phosphorus diamide **36** under conditions developed by Hanessian in the total synthesis of ambruticin S (Scheme 5).<sup>19</sup> The olefination provided a 15 : 1 mixture of alkene isomers which, after silyl deprotection, were separated to afford the desired *E*-alkene **38** in 39% yield over the two steps. Finally, conversion of alcohol **38** to the corresponding phenyl tetrazole sulfone **11** (fragment 3) proceeded smoothly through a sequence of Mitsunobu coupling and subsequent oxidation of the intermediate sulfide. The total synthesis of 20,21-dihydroambruticin F (**9**) was completed as shown in

Scheme 5. Deprotonation of sulfone **11** with 1.2 equivalents of KHMDS in DME, followed by treatment with 1.2 equivalents of aldehyde **10** gave an inseparable mixture of alkene isomers ( $E/Z = 10 : 1$ ) in 40% yield. The use of NaHMDS in a mixture of THF and HMPA resulted in an improved yield of 78% for the required coupling but reduced the stereoselectivity ( $E/Z = 3 : 1$ ). A screen of further solvents and bases failed to improve either the yield or selectivity. Silyl deprotection of **39** with TBAF followed by hydrolysis of the ethyl ester gave the target, 20,21-dihydroambruticin F (**9**).

The same modular strategy was used for the synthesis of ambruticin F (**2**). In this case the known sulfone **14** (ref. 20) was coupled to aldehyde **10** to afford alkene **41** in 38% yield as a 10 : 1 mixture of inseparable *E/Z* isomers (Scheme 6). Again, it was found that use of NaHMDS in a mixture of THF and HMPA in the coupling reaction gave an improved yield (80%) but the selectivity was 3 : 1 in favour of the *E*-alkene. Deprotection of bis-silyl ether **41** with TBAF in THF followed by ester hydrolysis completed the first total synthesis of ambruticin F (**2**). As NMR



Scheme 6 Completing the total syntheses of ambruticins F and S.



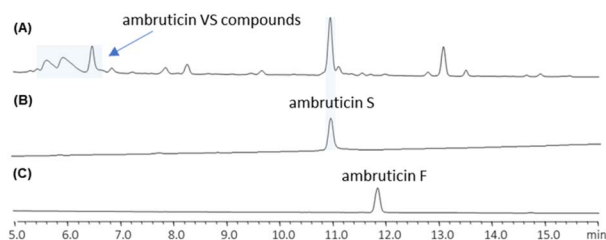


Fig. 1 HPLC traces of (A) wild-type *S. celluloseum* So ce10, (B) synthetic standard of ambruticin S (4) and (C) synthetic standard of ambruticin F (2).

data of the natural product 2 were not available for comparison with the synthetic material, we aimed to convert 2 to a fully characterised metabolite.

Further variations in the structures of the ambruticins arise from the presence of different groups at C-5, for example ambruticin S (4) has a 5 $\beta$ -alcohol rather than the 5 $\alpha$ -alcohol proposed to be present in ambruticin F (2). Spectral data have been reported for the natural product ambruticin S (4) and it has been a target for total synthesis.<sup>15–19</sup> To correlate our synthetic ambruticin F with ambruticin S, a biomimetic oxidation/reduction sequence was undertaken (Scheme 6).<sup>22</sup> Reaction of dihydroxy ester 42 with Fétizon's reagent ( $\text{Ag}_2\text{CO}_3$  on Celite) led to selective oxidation of the 5-axial alcohol to ketone 43 in 54% yield, whereas with DMP in DCM the ketone was isolated in only 33% yield.<sup>14,38</sup> Reduction of ketone 43 with  $\text{NaBH}_4$  in MeOH gave a separable mixture of 1,2-*syn*-diol (ambruticin F ethyl ester 42) in 35% yield and 1,2-*anti*-diol (ambruticin S ethyl ester) in 47% yield. Finally, hydrolysis of the ethyl ester of ambruticin S completed the total synthesis of ambruticin S (4), and all spectral data were consistent with those reported for the natural product as well as products from previous total syntheses (ESI, Fig. S5 and S6†).<sup>17,19,38</sup>

### Engineering the ambruticin biosynthetic pathway

We found that cultures of the wild-type strain of *S. celluloseum* So ce10 produce predominantly ambruticin S and the VS series of compounds, and ambruticin F could not be detected by LC-MS in culture extracts (Fig. 1A). Hence, to investigate production of both ambruticin F (2) and 20,21-dihydroambruticin F (9), it was necessary to engineer the biosynthetic pathway in *S. celluloseum* So ce10.

Strains of the genus *Sorangium* are, however, very slow growing, notoriously difficult to ferment and challenging to genetically engineer. Gene disruption of So ce10 has only been successfully achieved by Reeves and co-workers in 2006 and since then no further genetic engineering of this strain has been reported.<sup>22</sup> In their study, target genes were disrupted through conjugation of a plasmid that could insert into the middle of the gene by a single recombination event. Mutants generated by this method could potentially undergo a second homologous recombination event and revert to the wild-type. To circumvent the challenges of conjugation and lability of mutants obtained, we developed an efficient electroporation method for transferring DNA into So ce10 cells and introduced a plasmid that

contains an antibiotic selection marker flanked by upstream and downstream fragments of the target gene. This superior approach led to far more stable mutant strains generated via a double crossover recombination event.

Previous studies had shown that disrupting *ambQ* from the ambruticin biosynthetic gene cluster led to accumulation of ambruticin F but along with ambruticin S and the VS series of compounds found in the wild-type strain, potentially due to the function of AmbQ being complemented by AmbN.<sup>22</sup> This led us to propose that disruption of both *ambQ* and *ambN*, as well as other downstream genes, would afford ambruticin F as the major metabolite. Therefore, the  $\Delta\text{ambN-S}$  mutant strain of *S. celluloseum* So ce10 was constructed by replacing the continuous region of *ambN*, *ambQ*, *ambR* and *ambS* genes with a hygromycin selection marker (Fig. 2A). Fermentation of the  $\Delta\text{ambN-S}$  mutant gave ambruticin F as the major product which was isolated and characterised (Fig. 2B). The NMR data of the purified natural ambruticin F matched perfectly with those of the synthetic sample confirming the structure of the natural product (ESI, Fig. S3 and S4†).

Reeves proposed that 20,21-dehydrogenation of THPs to DHPs in the ambruticins is catalysed by the two-component enzyme system including the Rieske oxygenase AmbP and the NAD(P)/FAD-dependent oxidoreductase AmbO and indicated that this intriguing selective desaturation may occur at various points in the biosynthetic pathway.<sup>22</sup> To investigate whether these enzymes could indeed be implicated in the conversion of 20,21-dihydroambruticin F to ambruticin F, cultures of *S. celluloseum* So ce10 were grown in which the continuous region of *ambP*, *ambO*, *ambN*, *ambQ*, *ambR* and *ambS* genes (designated as the  $\Delta\text{ambP-S}$  mutant) were disrupted. Analysis of the crude extract by HPLC (Fig. 2C) revealed one major product which was isolated and NMR analysis and comparison with synthetic material confirmed that 20,21-dihydroambruticin F (9) had accumulated. Similar to the  $\Delta\text{ambP-S}$  mutant in which the *ambP* and *ambO* genes were deleted together, deletions of *ambP* and *ambO* individually from the  $\Delta\text{ambN-S}$  mutant, designated as  $\Delta\text{ambN-S}/\Delta\text{ambP}$  and  $\Delta\text{ambO-S}$  respectively, also yielded 9 as the major metabolite (ESI, Fig. S1 and S2†). These studies fully support the important role of AmbP and AmbO as the key enzymes involved in desaturation of tetrahydropyrans leading to 20,21-alkenes in ambruticin biosynthesis.

In a parallel experiment, deletions of the *jerP* and *jerO* genes were carried out in the closely related jerangolid biosynthetic pathway in *S. celluloseum* So ce307 (Fig. 3A). Both JerP and JerO share 78% sequence identity to AmbP and AmbO.<sup>22</sup> Compared with the production of jerangolid A (44) by wild-type *S. celluloseum* So ce307, both the  $\Delta\text{jerP}$  and  $\Delta\text{jerO}$  mutants produced jerangolid H (45) lacking the 13,14-double bond as the major compound (Fig. 3B).

With trisubstituted tetrahydropyrans 20,21-dihydroambruticin F (9) and jerangolid H (45) in hand, we next turned to biotransformation assays with AmbP and AmbO. Despite various attempts, no clear turnover was observed with either purified enzymes of AmbP and AmbO or their expressing *E. coli* whole cells. We therefore further engineered the  $\Delta\text{ambN-S}$  mutant strain and deleted all other ambruticin biosynthetic





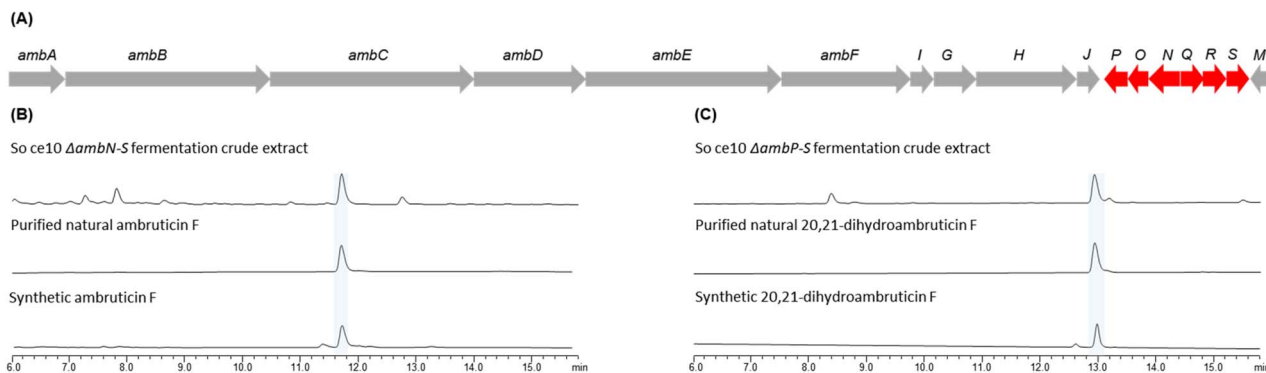


Fig. 2 (A) Organisation of the amburcicin biosynthetic gene cluster where genes disrupted in this study are highlighted in red. (B) HPLC traces of the  $\Delta ambN$ -S mutant of *S. cellulorum* So ce10 compared with synthetic standard of amburcicin F (2). (C) HPLC traces of the  $\Delta ambP$ -S mutant of *S. cellulorum* So ce10 compared with synthetic standard of 20,21-dihydroamburcicin F (9).

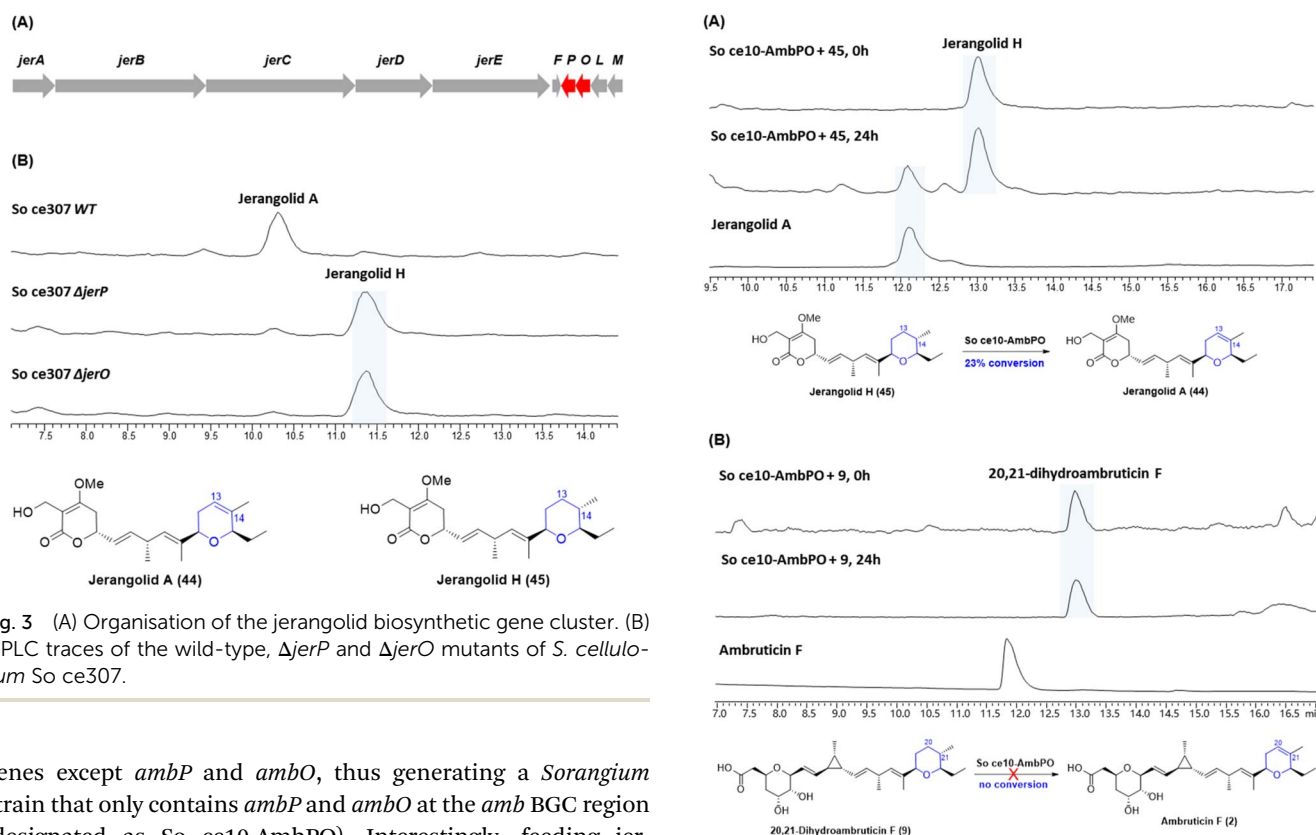


Fig. 3 (A) Organisation of the jerangolid biosynthetic gene cluster. (B) HPLC traces of the wild-type,  $\Delta jerP$  and  $\Delta jerO$  mutants of *S. cellulorum* So ce307.

genes except *ambP* and *ambO*, thus generating a *Sorangium* strain that only contains *ambP* and *ambO* at the *amb* BGC region (designated as So ce10-AmbPO). Interestingly, feeding jerangolid H to this *Sorangium* strain showed conversion to jerangolid A (Fig. 4A), whereas 20,21-dihydroamburcicin F (9) was recovered unchanged in an analogous feeding experiment with So ce10-AmbPO (Fig. 4B). These results are inconsistent with the original proposal that the desaturation step may occur late in the biosynthetic pathway.<sup>22</sup> Bearing in mind that amburcicin J (1) with the 20,21-alkene has been isolated from the  $\Delta ambJ$  mutant,<sup>22</sup> desaturation is now proposed to happen at an earlier stage of the biosynthetic pathway, most likely before the western THP ring is formed.

Note: During the review process of this manuscript, Guth *et al.* reported reconstitution of the activity of JerP and JerO by extensive optimisation of the whole-cell biotransformation

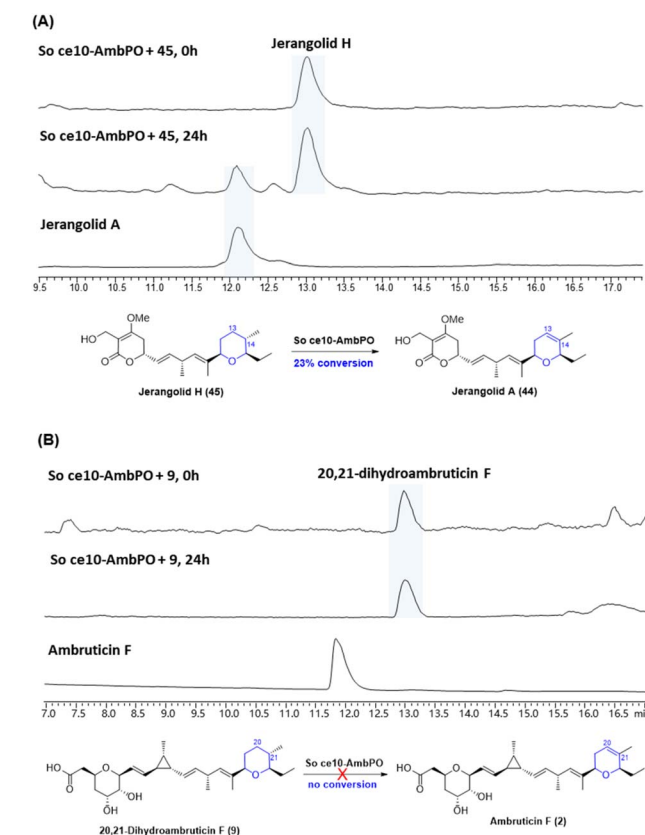


Fig. 4 (A) Biotransformation of jerangolid H (45) by So ce10-AmbPO. (B) Biotransformation of 20,21-dihydroamburcicin F (9) by So ce10-AmbPO.

conditions in *E. coli*, similar conversion of jerangolid H to jerangolid A was observed.<sup>39</sup>

## Conclusions

In summary, we have completed the first total synthesis of 20,21-dihydroamburcicin F (9), whereby three fragments were combined by two Julia-Kocienski olefinations. The two THP



rings were constructed on multi-gram scales by a biomimetic epoxidation–cyclisation strategy for the C1–C8 fragment and a Prins cyclisation for the second ring. The modular approach was readily adapted to allow completion of the first total synthesis of ambruticin F (2) which in turn was converted to ambruticin S (4). These synthetic studies provided key standards to enable investigation of dihydropyran formation in ambruticin biosynthesis. Cultures of wild-type *S. cellulorum* So ce10 produced mainly ambruticin S and the VS series of metabolites. A method was developed to carry out gene knockout experiments reliably which revealed that the  $\Delta ambP$ -S mutant of *S. cellulorum* accumulated the novel bisTHP polyketide 20,21-dihydroambruticin F whilst the  $\Delta ambN$ -S mutant gave ambruticin F with the 20,21-alkene as the major metabolite. Similar results were obtained when *ambP* and *ambO* were deleted individually in these strains. These studies confirm that AmbP and AmbO (a Rieske enzyme and flavin-dependent monooxygenase respectively) are implicated in 20,21-alkene formation. Furthermore, the results of feeding studies with *Sorangium* strains containing only *ambP* and *ambO* are in accord with desaturation occurring prior to formation of the C3–C7 tetrahydropyran in ambruticin biosynthesis, laying the foundation for future investigations into the timing and mechanism of this intriguing biotransformation.

## Data availability

All the data supporting this article have been included in the ESI.†

## Author contributions

MPC, LW and CLW co-ordinated the project. JIB and BR conducted all the synthetic work (under the supervision of CLW) and XZ and KG completed all the biosynthetic studies (under the supervision of LW). JIB, MPC, LW and CLW wrote the manuscript.

## Conflicts of interest

There are no conflicts to declare.

## Acknowledgements

We thank the EPSRC Bristol Chemical Synthesis Centre for Doctoral Training (EP/L015366/1) for a studentship to JIB and the National Key R&D Program of China (2021YFC2100500), National Natural Science Foundation of China (32270083) to LW.

## Notes and references

- 1 S. M. Ringel, R. C. Greenough, S. Roemer, D. Connor, A. L. Gutt, B. Blair, G. Kanter and M. Von Strandtmann, *J. Antibiot.*, 1977, **30**, 371.
- 2 F. Hahn and F. M. Guth, *Nat. Prod. Rep.*, 2020, **37**, 1300.
- 3 V. Michelet and J.-P. Genet, *Curr. Org. Chem.*, 2005, **9**, 405.
- 4 S. Shadomy, C. J. Utz and S. White, *Antimicrob. Agents Chemother.*, 1978, **14**, 95.
- 5 P. Knauth and H. Reichenbach, *J. Antibiot.*, 2000, **53**, 1182.
- 6 H. B. Levine, S. M. Ringel and J. M. Cobb, *Chest*, 1978, **73**, 202.
- 7 M. C. Fisher, A. Alastruey-Izquierdo, J. Berman, T. Bicanic, E. M. Bignell, P. Bowyer, M. Bromley, R. Brüggemann, G. Garber, O. A. Cornely, S. J. Gurr, T. S. Harrison, E. Kuijper, J. Rhodes, D. C. Sheppard, A. Warris, P. L. White, J. Xu, B. Zwaan and P. E. Verweij, *Nat. Rev. Microbiol.*, 2022, **20**, 557.
- 8 F. Bongomin, S. Gago, R. Oladele and D. Denning, *J. Fungi*, 2017, **3**, 57.
- 9 V. S. Brauer, C. P. Rezende, A. M. Pessoni, R. G. De Paula, K. S. Rangappa, S. C. Nayaka, V. K. Gupta and F. Almeida, *Biomolecules*, 2019, **9**, 521.
- 10 M. C. Fisher, N. J. Hawkins, D. Sanglard and S. J. Gurr, *Science*, 2018, **360**, 739.
- 11 A. Casadevall, *Pathog. Immun.*, 2018, **3**, 183.
- 12 S. E. Greenspan, D. S. Bower, E. A. Roznik, D. A. Pike, G. Marantelli, R. A. Alford, L. Schwarzkopf and B. R. Scheffers, *Sci. Rep.*, 2017, **7**, 9349.
- 13 M. C. Fisher, D. A. Henk, C. J. Briggs, J. S. Brownstein, L. C. Madoff, S. L. McCraw and S. J. Gurr, *Nature*, 2012, **484**, 186.
- 14 D. T. Connor and M. V. Strandtmann, *J. Org. Chem.*, 1978, **43**, 4606.
- 15 A. S. Kende, Y. Fujii and J. S. Mendoza, *J. Am. Chem. Soc.*, 1990, **112**, 9645.
- 16 T. A. Kirkland, J. Colucci, L. S. Geraci, M. A. Marx, M. Schneider, D. E. Kaelin and S. F. Martin, *J. Am. Chem. Soc.*, 2001, **123**, 12432.
- 17 P. Liu and E. N. Jacobsen, *J. Am. Chem. Soc.*, 2001, **123**, 10772.
- 18 E. Lee, S. J. Choi, H. Kim, H. O. Han, Y. K. Kim, S. J. Min, S. H. Son, S. M. Lim and W. S. Jang, *Angew. Chem., Int. Ed.*, 2002, **41**, 176.
- 19 S. Hanessian, T. Focken, X. Mi, R. Oza, B. Chen, D. Ritson and R. Beaudegnies, *J. Org. Chem.*, 2010, **75**, 5601.
- 20 J. I. Bowen, L. Wang, M. P. Crump and C. L. Willis, *Org. Biomol. Chem.*, 2021, **19**, 6210.
- 21 K. Trentadue, C. Chang, A. Nalin and R. E. Taylor, *Chem.–Eur. J.*, 2021, **27**, 11126.
- 22 B. Julien, Z.-Q. Tian, R. Reid and C. D. Reeves, *Chem. Biol.*, 2006, **13**, 1277.
- 23 G. Berkhan and F. Hahn, *Angew. Chem., Int. Ed.*, 2014, **53**, 14240.
- 24 J. I. Bowen, L. Wang, M. P. Crump and C. L. Willis, *Org. Biomol. Chem.*, 2022, **20**, 1150.
- 25 T. Hollmann, G. Berkhan, L. Wagner, K. H. Sung, S. Kolb, H. Geise and F. Hahn, *ACS Catal.*, 2020, **10**, 4973.
- 26 P. R. Blakemore, *J. Chem. Soc., Perkin Trans. 1*, 2002, **2**, 2563.
- 27 M. B. Hodge and H. F. Olivo, *Tetrahedron*, 2004, **60**, 9397.
- 28 T. E. Smith, M. Djang, A. J. Velander, C. W. Downey, K. A. Carroll and S. van Alphen, *Org. Lett.*, 2004, **6**, 2317.
- 29 K.-M. Chen, G. E. Hardtmann, K. Prasad, O. Repić and M. J. Shapiro, *Tetrahedron Lett.*, 1987, **28**, 155.



- 30 S. D. Rychnovsky, B. Rogers and G. Yang, *J. Org. Chem.*, 1993, **58**, 3511.
- 31 Y. Gao, J. M. Klunder, R. M. Hanson, H. Masamune, S. Y. Ko and K. B. Sharpless, *J. Am. Chem. Soc.*, 1987, **109**, 5765.
- 32 K. Jeyakumar, R. D. Chakravarthy and D. K. Chand, *Catal. Commun.*, 2009, **10**, 1948.
- 33 S. Higashibayashi, K. Shinko, T. Ishizu, K. Hashimoto, H. Shirahama and M. Nakata, *Synlett*, 2000, **2000**, 1306.
- 34 C. Olier, M. Kaafarani, S. Gastaldi and M. P. Bertrand, *Tetrahedron*, 2010, **66**, 413.
- 35 V. K. Yadav, A. K. Verma, P. Kumar and V. Hulikal, *Chem. Commun.*, 2014, **50**, 15457.
- 36 J. Pospíšil, T. Kumamoto and I. E. Markó, *Angew. Chem., Int. Ed.*, 2006, **45**, 3357.
- 37 R. H. Crabtree and M. W. Davis, *J. Org. Chem.*, 1986, **51**, 2655.
- 38 D. T. Connor, R. C. Greenough and M. Von Strandtmann, *J. Org. Chem.*, 1977, **42**, 3664.
- 39 F. M. Guth, F. Lindner, S. Rydzek, A. Peil, S. Friedrich, B. Hauer and F. Hahn, *ACS Chem. Biol.*, 2023, **18**, 2450.

